ChemComm

Accepted Manuscript

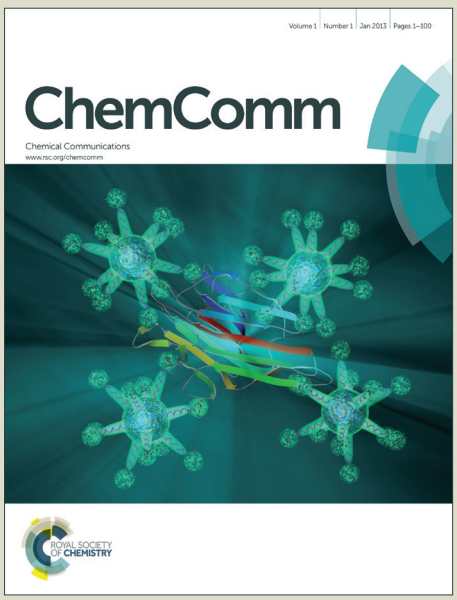

ROYAL SOCIETY OF CHEMISTRY

www.rsc.org/chemcomm

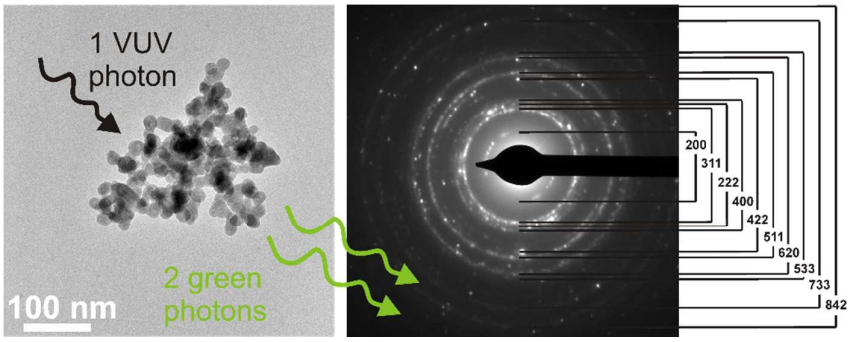

Green quantum cutting can be achieved in nanoscale materials irrespective of a large surface and other killer traps.

Journal Name

RSCPublishing

COMMUNICATION

Quantum cutting in nanoparticles producing two green photons

Cite this: DOI: 10.1039/x0xx00000x

C. Lorbeer[a] and A.-V. Mudring[a,b*]

Received 00th January 2012,
Accepted 00th January 2012

DOI: 10.1039/x0xx00000x

www.rsc.org/

A synthetic route to nanoscale $NaGdF_4$:Ln is presented which allows for quantum cutting based on the Gd-Er-Tb system. This shows, that cross-relaxation and other energy transfer processes necessary for multiphoton emission can be achieved in nanoparticles even if the large surface and the potentially huge amount of killer traps would suggest a lack of subsequent emission.

The development of multiphoton-emitting luminescent materials, which produce more than one visible photon per incident VUV, UV, visible or NIR photon, can significantly improve the overall energy conversion of devices such as solar cells, fluorescent lamps or plasma display panels.[1-4] Phosphors generating more than one photon after absorbing one, are called *quantum cutters*. Intrinsically, such phosphors may show a quantum yield above 100 %. Apart from their potential for applications, the study of quantum cutting materials is of great interest as energy transfer processes can be studied. Energy transfer processes in doped luminescent materials are strongly dependent on the local structure surrounding the optical center.[5] Studying the energy transfer processes in detail may yield valuable information on how a material has to be constructed if quantum cutting should occur. Particularly nanoscale materials are of great interest, as the applicability of such materials is straightforward, minimizes processing constraints and has been shown to enable new benchmarks in material science. [6,7]

In contrast to the Gd^{3+}-Eu^{3+} quantum cutting pair which delivers two red photons, the corresponding green-emitting process involves three ions, Gd^{3+}, Er^{3+} and Tb^{3+}, between which energy transfer is required. As a result, it appears to be more complex and difficult and, thus, is far less studied. The underlying energy transfer mechanism as schematically shown in Fig. 1 was proposed by Meijerink et al. and experimentally proven on single crystalline materials.[8, 9] Compared to the Gd^{3+}-Eu^{3+} quantum-cutting pair, immediately a tremendous advantage of this process compared to the Gd-Eu pair falls into the eyes: Efficient absorption of UV radiation by excitation into the fd level of Er^{3+} instead of excitation into levels involving forbidden electric dipole transitions and therefore extremely weak f-f transitions. This absorption into the fd level of Er^{3+} is followed by a cross-relaxation step leading to Er^{3+} in the $^4S_{3/2}$ state and promotion of a Gd^{3+} ion from the ground state to the ^6D_J excited state. The energy of the excited Gd^{3+} ion is then transferred over the Gd^{3+} sublattice via energy migration, while the Er^{3+} in the $^4S_{3/2}$ state decays radiatively to the ground state emitting the first green photon. Then, the energy of the excited Gd^{3+} ion is transferred to a Tb^{3+} ion, followed by non-radiative relaxation to the $^5D_3$ and $^5D_4$ excited states. The emission of a second green photon is possible from both levels to the ground state, although the $^5D_4 \rightarrow {}^7F_J$ transitions are usually dominating. Thus, two green photons (one by Er^{3+} and one by Tb^{3+}) are emitted upon excitation of one VUV photon.

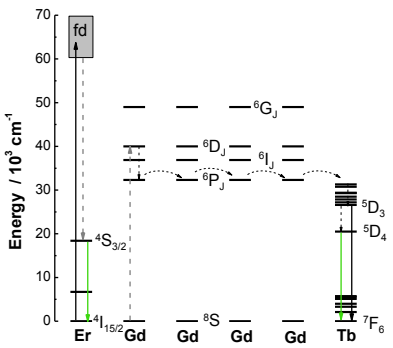

Figure 1. Schematic energy level diagram showing the quantum cutting mechanism in the Gd-Er-Tb system. Some transitions are left out for clarity. The cross-relaxation process is depicted by dashed grey arrows, while the black dashed arrows indicate non-radiative energy transfer or relaxation processes. Adapted from [8].

To achieve quantum cutting in the nanoscale would open up a interest in this topic of enormous potential. Quantum cutting in applicable materials such as nanoparticles is, to the best of our knowledge, not yet reported for the Er-Tb couple. The more common, but externally less-efficient Gd-Eu couple was reported also only a few times and the majority of publications on this topic were reported by us. Although experimental quantum cutting is known since 1999 (it was predicted already in the fifties), it was reported for the first time in nanoscale materials almost a decade after. Indeed, achieving cross-relaxation and other energy transfer processes necessary for multiphoton emission is not straightforward and requires exact control of the synthesis conditions and ubiquitous care about possible impurities of physical or chemical nature. The large surface of nanoparticles and the potentially huge amount of killer traps often promote quenching and thus render the realization of quantum cutting in the nanoscale and extraordinary difficult task as many factors have to be considered, controlled and mastered.

The complexity of the energy transfer mechanism requiring a special ion distribution in the host lattice is reflected by the fact that we were not able to obtain green quantum cutting material by our recently established synthesis method which was greatly successful to obtain minute, oxygen-free fluoride nanoparticles,[10, 11] that showed tremendously high quantum yields for the Gd^{3+}-Eu^{3+} quantum cutting pair. The synthesis of $NaGdF_4$ was not possible via the established reaction. Therefore, we decided to assess a different synthesis route to ternary fluorides [12] and optimize it to yield uniform nanoscale particles. In a typical reaction, sodium acetate and lanthanide acetate hydrates (gadolinium, erbium, terbium) were mixed in desired amounts. The mixture was then dispersed in the ionic liquid 1-butyl-3-methylimidazolium tetrafluoroborate ($[C_4mim](BF_4)$) by stirring for 2 h under inert atmosphere in order to remove any oxygen. Then the reaction dispersion is heated in a laboratory microwave to 60 °C for five minutes, followed by raising the temperature to 200 °C for only five minutes. The first heating step is mandatory to achieve a uniformly distributed dispersion leading to a uniform, complete conversion of the reaction material. Employing microwave radiation is compulsory as it leads to high nucleation rates and in consequence minute particles.

The sample identifier and the corresponding dopant ion concentrations are listed in Table 1. The amount of Er^{3+} and particularly of Tb^{3+} has to be kept low to prevent direct transfer processes between the ions, although for efficient absorption a higher amount of Er^{3+} ions is desirable. However, low dopant concentrations could be problematic in nanoparticles as usually stronger emission is obtained with larger amounts of optically active ions in comparison to the concentrations used in bulk materials and single crystals.[13] To balance all the effects, $NaGdF_4$ particles with overall dopant concentrations of 1.1% and 1.8% were synthesized, wherein the Tb^{3+} concentration is kept as low as 0.1% or 0.3 %.

Table 1. Sample identifier.

Sample identifier	Er^{3+}/ %	Tb^{3+} / %	Particle size
ErTb1	1.0	0.1	7.8 ± 1.0 nm
ErTb2	1.5	0.3	8.1 ± 1.0 nm

The powder X-ray diffraction patterns reveal the as-prepared material to crystallize in the cubic $NaGdF_4$ structure. No distinct phase of the starting materials or the simple fluorides NaF or GdF_3 nor any other crystalline phase are observable. The particle sizes were calculated according to the Scherrer equation and amount to 7.8 nm for ErTb1 and 8.1 nm for ErTb2.

Transmission electron microscopy suggests a larger particle size of 19.4 ± 4.2 nm in average. While the Scherrer equation estimated the extension of one crystalline domain, one particle may consist of more than one domain. This could explain the deviation in particle size determination with both methods. Indeed, the electron diffraction pattern confirmed the polycrystalline nature of the particles (see Supporting Information figure 1). The particles observable on the TEM micrographs are uniform, loosely clustered particles of spherical and cuboidal shape.

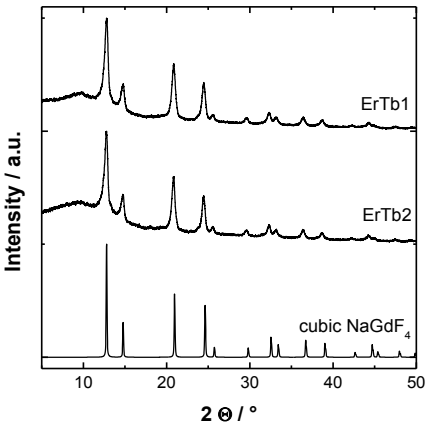

Figure 2. Powder X-ray diffraction pattern of the synthesized $NaGdF_4$: Er, Tb particles. The database pattern of cubic $NaGdF_4$ (simulated from ICSD60257 cubic phase of $NaYF_4$, lattice constants of $NaGdF_4$ from PDF-2 [27-697]) is shown for comparison.

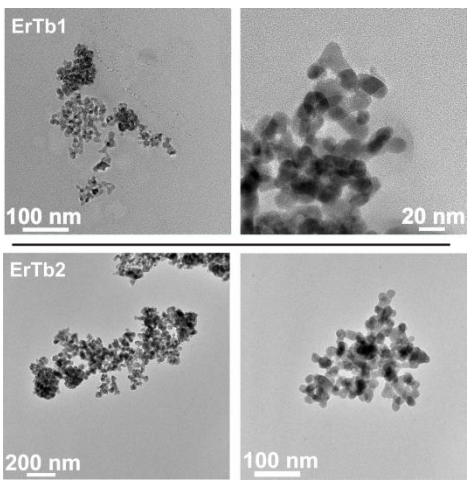

Figure 3. Representative TEM micrographs of the synthesized $NaGdF_4$:Er^{3+}, Tb^{3+} particles with different dopant concentrations.

The luminescence spectra consist of the typical f-f transitions of Er^{3+} and Tb^{3+}. Irrespective of the excitation wavelengths λ_{ex}= 377 nm or 274 nm, the same emission spectra are obtained. To study the quantum cutting abilities, VUV excited emission spectra were recorded and displayed in figure 4. For this purpose, excitation at λ_{ex} = 145 nm into the fd level of Er^{3+} and at 274nm into Gd^{3+} were

carried out. The quantification of the quantum cutting process is similar to the Gd-Eu process: Emission spectra exciting directly in the fd states of Er^{3+}, where quantum cutting can occur, and exciting into low lying Gd^{3+} levels, where the energy is not sufficient to allow the splitting of one photon into two visible photons, have to be recorded. Thereby, the excitation into Gd^{3+} serves as reference. The excitation into Er^{3+} can be followed by two extremes: On the one hand, direct and complete energy transfer to Gd^{3+} could occur. In this case, the emission spectrum equals the emission obtained after direct Gd^{3+} excitation. On the other hand, with the cross-relaxation step, which is mandatory for quantum cutting, additional Er^{3+} lines will occur due to the radiative relaxation of Er^{3+} from the $^4S_{3/2}$ level. Hence, the quantum cutting efficiency can be estimated from the increase in Er^{3+} emission when excited into Er^{3+} compared to the emission obtained via excitation in Gd^{3+}:[8]

$$\frac{p_{ET+}}{p_{ET+} + p_{ET-}} = \frac{R(\frac{^4S_{3/2}}{rest})_{Er^{3+}} - R(\frac{^4S_{3/2}}{rest})_{Gd^{3+}}}{R(\frac{^4S_{3/2}}{rest})_{Gd^{3+}} + 1}$$

where p_{ET+} and p_{ET-} are the probabilities of the desired and unwanted energy transfer processes, respectively. R is the ratio of the $^4S_{3/2}$ transition of Er^{3+} compared to all other transitions (including Tb^{3+}, Gd^{3+}, and other Er^{3+} transitions) excited into Gd^{3+} or Er^{3+}.

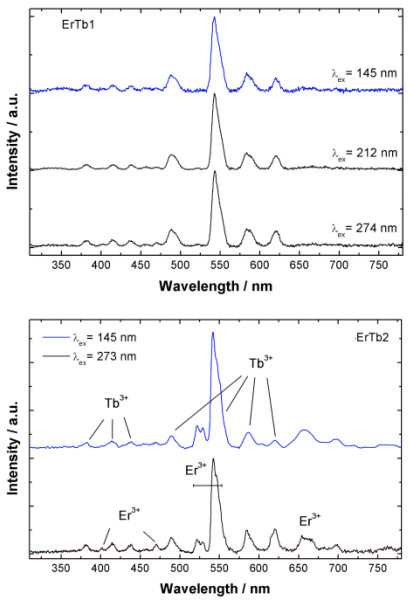

Figure 4. Room temperature emission spectra of the $NaGdF_4$: Er^{3+}, Tb^{3+} particles synthesized with different dopant concentrations.

In case of the lower concentrated ErTb1 particles, the emission spectra are similar independent from the excitation wavelength and thus no quantum cutting was obtained. In case of ErTb2, a significant increase of the $^4S_{3/2} \rightarrow {}^4I_{15/2}$ transition is recorded and the quantum cutting efficiency was calculated to amount to 122 %, which is close to the limit suggested by Meijerink et al.[8] To the best of our knowledge, this is the first report on Er-Gd-Tb quantum cutting in nanoscale materials. Although the quantum cutting efficiency is limited, the cross-relaxation and other energy transfer mechanism can be achieved in nanoparticles even if the large surface and the potentially huge amount of killer traps suggests a lack of subsequent emission. Particularly with regard to Gd^{3+} containing phosphors, where energy migration over the whole sublattice can efficiently occur, quantum cutting effects on the nanoscale are surprising and extremely appealing for fundamental science, for understanding the energy transfer and corresponding radiative relaxation mechanism, and even for potential applications.

Conclusions

In summary, with the successful preparation of $NaGdF_4$ particles doped with Er^{3+} and Tb^{3+} it has been confirmed for the first time that this kind of quantum cutting process relying on multiple energy transfers (as previously only reported for bulk materials) can also be observed in nanomaterials < 10 nm despite their tremendously high surface.

Acknowledgment

This work was supported in part by the Critical Materials Institute, an Energy Innovation Hub funded by the U.S. Department of Energy, Office of Energy Efficiency and Renewable Energy, Advanced Manufacturing Office and the European Research Council with an ERC starting grant ("EMIL", contract no. 200475). A.-V. M. thanks the Fonds der Chemischen Industrie for a Dozentenstipendium, C. L. thanks the Fonds der Chemischen Industrie for a doctoral scholarship. DESY (proposal no. II-20090181) is acknowledged for access to synchrotron facilities.

Notes and references

[a] Inorganic Chemistry III- Materials Engineering and Characterization, Ruhr-Universität Bochum, Universitätsstr. 150, 44801 Bochum, Germany.

[b] Department of Materials Science and Engineering, Iowa State University and Critical Materials Institute, Ames Laboratory (DOE), Ames, IA 50010, USA. E-mail: mudring@iastate.edu

Electronic Supplementary Information (ESI) available: Experimental and instrumental details, and electron diffraction pattern. See DOI: 10.1039/c000000x/

1 J. J. Eilers, D. Biner, J. T. van Wijngaarden, K. Krämer, H.-U. Güdel, A. Meijerink, *Appl. Phys. Lett.*, 2010, **96**, 151106.
2 S. Lepoutre, D. Boyer, R. Mahiou, *J. Lumin*., 2008, **128**, 635.
3 B. M. van der Ende, L. Aarts, A. Meijerink, *Adv. Mater.*, 2009, **21**, 3073.
4 R. T. Wegh, H. Donker, K. D. Oskam, A. Meijerink, *Science*, 1999, **283**, 663.
5 M. Karbowiak, A. Mech, A. Bednarkiewicz, W. Strek, L. Kpiński, *J. Phys. Chem. Solids*,, 2005, ***66***, 1008.
6 H. Song, P. A. Tanner, *Doped Nanomaterials and Nanodevices*, Vol. 1 (Ed.: W. Chen), American Scientific Publishers, Valencia, **2010**.
7 E. Garnett, P. Yang, *Nano Lett.*, 2010, **10**, 1082.
8 R. T. Wegh, E. V. D. van Loef, A. Meijerink, *J. Lumin.*, 2000, **90**, 111.
9 B. Moine, L. Beauzamy, P. Gredin, G. Wallez, J. Labeguerie, *Opt. Mater*., 2008, **30**, 1083.

10 C. Lorbeer, J. Cybinska, A.-V. Mudring, *Chem. Commun.*, 2010, **46**, 571.
11 C. Lorbeer, J. Cybinska, A.-V. Mudring, *J. Mater. Chem. C*, 2014, **2**, 1862.
12 C. Chen, L.-D. Sun, Z.-X. Li, L.-L. Li, J. Zhang, Y.-W. Zhang, C.-H. Yan, *Langmuir*, 2010, **26**, 8797.
13 A. Bednarkiewicz, A. Mech, M. Karbowiak, W. Strek, *J. Lumin.*, 2005, **114**, 247.

